Treatment of Aqueous Arsenite Using Modified Biomass-Based Sorbent

Khaled Zoroufchi Benis, Kerry McPhedran, and Jafar Soltan

Abstract The occurrence of high concentrations of arsenic (As) in water has been recognized as a global health and environmental problem. Sorption is regarded as a promising As treatment method due to its simplicity and potential for high efficiency. Canada has a strong agricultural industry that produces waste products that can be converted to value-added products. Considering the availability of agricultural residue in Canada, the cost of the sorption process can be decreased by using agricultural residue-based sorbents (biosorbents) as an eco-friendly alternative for commercial sorbents. In this study, sorption of arsenite, As(III), from aqueous solutions onto Fe oxide-modified canola straw (MCS) was investigated. The results showed that the negligible As(III) sorption capacity of raw canola straw increased significantly to 791 μg/g after modification in the removal of As(III) from a 1000 μg/L solution. Studying the effect of solution pH showed that As(III) sorption capacity of MCS increased by increasing the solution pH from 3 to 10. A kinetic study showed that about 66% of the ultimate sorption capacity was reached within four hours. The sorption kinetic data was best represented by pseudo-second-order and Elovich models suggesting that chemisorption may be the rate-determining step of the sorption process. The isothermal data of As(III) sorption followed Freundlich and Redlich–Peterson models indicating a hybrid adsorption mechanism with a higher probability of a multilayer heterogeneous adsorption. Studying the effect of co-existing anions in the solution upon the As(III) removal efficiency of MCS indicated a significant antagonistic impact of selenate (SeO_4^{2-}), selenite (SeO_3^{2-}), and phosphate (PO_4^{3-}). However, the effect of nitrate (NO_3^-) and chloride (Cl^-) on As(III)

K. Zoroufchi Benis · J. Soltan
Department of Chemical and Biological Engineering, University of Saskatchewan, Saskatoon, SK, Canada

K. McPhedran (✉)
Department of Civil, Geological and Environmental Engineering, University of Saskatchewan, Saskatoon, SK, Canada
e-mail: kerry.mcphedran@usask.ca

K. Zoroufchi Benis · K. McPhedran · J. Soltan
Global Institute for Water Security, University of Saskatchewan, Saskatoon, SK, Canada

R. Gupta et al. (eds.), *Proceedings of the Canadian Society of Civil Engineering Annual Conference 2022*, Lecture Notes in Civil Engineering 363,
https://doi.org/10.1007/978-3-031-34593-7_61

removal efficiency was insignificant, indicating that inner-sphere complexation was the leading mechanism in As(III) sorption.

Keywords Arsenite · Biosorption · Canola straw · Co-existing ions

1 Introduction

Arsenic (As) is a toxic and carcinogenic metalloid and exists ubiquitously in nature. The World Health Organization (WHO) has acknowledged As contamination as a "major public health issue" [1]. The As poisoning from drinking contaminated waters is the main route of As exposure for humans [2] with source natural waters having a wide range of As concentrations from 0.5 to 5000 μg/L [3]. WHO guidelines indicate a maximum As concentration of 10 μg/L in drinking water [4], and it has been reported that over 200 million people worldwide are exposed to As concentrations higher than this permissible level [5]. Prolonged exposure to As causes a variety of potentially lethal health problems by creating risks of different diseases such as cancer, melanosis, gangrene, hyperkeratosis, enlargement of liver, and black foot disease [6]. As occurs in four oxidation states [As(V), As(III), As(0), and As(−III)] in the natural environment and its toxicity and mobility in the environment depends on its oxidation state [7]. Generally, inorganic As compounds are more toxic compared to organic arsenics. Among these, arsenite, As(III), is the most toxic and harmful to human beings due to its higher mobility which also makes it more difficult to remove from contaminated waters [8].

The common As removal technologies are based on precipitation techniques followed by a separation system to remove insoluble As-bearing precipitates from water [9]. However, initial As concentration, target treatment concentration, oxidation state, and regulatory requirements are the key factors in the selection of an effective As removal method [10]. Therefore, the potential of different technologies such as filtration, reverse osmosis, membrane separation, and sorption for arsenic removal has been investigated in recent years [11]. Sorption has gained much attention among these technologies due to its cost effectiveness and easy operation [12]. The sorption performance of different materials such as activated carbon, resins, metal oxides, gels, minerals, and biomasses has been investigated for As removal [11, 13]. However, using many of these materials as As sorbents is not economically feasible [14]. Therefore, the consideration of using abundantly available ubiquitous agricultural residues for As sorption is of increasing interest [10]. Biosorption is a term that describes the removal of contaminants from aqueous solutions using biomass (e.g., agricultural residues).

Despite the abundance and low cost of agricultural residues, using them for As biosorption is not effective due to their low sorption capacities [15]. The low As sorption capacities of agricultural residues is due to the lack of appropriate chelating functional groups on their surface to complex with As and uptake it from aqueous solution.

Therefore, agricultural residues should be modified via deposition of suitable functional groups on their surface to make their sorption performance comparable with commercially available (but expensive) sorbents [16]. Generally, the biomasses can be activated by immersion in acid or alkaline solutions or they can be modified by deposition of modifying agents on their surface [10]. For example, Abid et al. [17] reported that the As(V) sorption capacity of orange peel biomass increased two times after treating the biomass with H_2SO_4 solution, which was attributed to the increased surface area of the treated biomass. Ebrahimi et al. [18] used $NaHCO_3$ for the treatment of wheat straw biomass. They found that As(V) sorption capacity of biomass increased from 54 to 108 μg/g after chemical treatment. Roy et al. [12] applied NaOH treatment on neem tree biomass followed by treatment in an H_2SO_4 solution and used the treated biomass for As(III) sorption. The As(III) sorption capacity of the modified biomass was 31 μg/g.

Although acid or alkali treatment of biomasses can improve their As sorption capacities, this improvement is limited because these treatments do not incorporate optimal functional groups for As sorption on the biomass surface [10]. However, Fe oxides have shown a high affinity for As ions [19], making them a popular agent in the modification of biomass for As biosorption [15]. For example, Tian et al. [20] modified wheat straw by deposition of Fe_3O_4 on straw particles. They reported that As sorption capacity of the modified biomass increased by increasing the amount of deposited Fe_3O_4. They also found that while the straw particles could not sorb As, the sorption capacity of Fe_3O_4/straw composite was higher than Fe_3O_4 alone. Hao et al. [21] developed a Fe-coated jute fiber biosorbent using a two-step process. First, the biomass surface was esterified with $C_4H_4O_3$ to graft with surface carboxyl groups to enhance Fe deposition. Then, $C_4H_4O_3$-treated biomass was modified with $Fe(NO_3)_3$ solution to form Fe oxyhydroxide on the surface of biomass. They observed an As(III) sorption capacity of 12.6 mg/g for the modified biosorbent. Meng et al. [22] reported that modification of orange peel using a mixed solution of $Fe(NO_3)_3$ and $Fe(NO_3)_2$ increased the surface area and As(V) sorption capacity of the biomass. However, As(V) reduced to more toxic As(III) during the sorption process by oxidation of deposited Fe(II) oxides on the surface to Fe(III) oxides.

Canola is a Canadian invention derived from rapeseed in the 1970s. Currently, Canada is the biggest global producer and exporter of canola, producing about 20 million tons of canola annually [23, 24]. Saskatchewan is the top province for canola production, contributing to about 55% of the total production in 2021 [23]. Considering the canola seeded area of 8.4 million ha in 2021 in Canada [23], and the average straw yield of 3 dry ton/ha [25], the total canola straw (CS) production can be estimated as 25.2 million ton/year. Using 60% of the produced CS for soil and livestock requirements [26], about 10 million ton/year would be available for other applications such as energy generation, chemical conversion, and production of other value-added products. Given the abundance of CS in Canada, it can be an appropriate precursor for the preparation of As biosorbent.

So far, the performance of chemically modified CS has been studied for the removal of As(V) from water [27], but there has yet to be investigation on its application for As(III) sorption. Therefore, this study aims to modify CS particles by deposition of Fe oxide using $FeCl_3$ solution and investigate the As(III) sorption performance of the modified CS (MCS). Additionally, the effect of co-existing ions, namely selenate (SeO_4^{2-}), selenite (SeO_3^{2-}), phosphate (PO_4^{3-}), nitrate (NO_3^-), and chloride (Cl^-), which could interfere with As(III) removal is investigated. Finally, a sorption mechanism has been proposed for the removal of As(III) by deposited Fe oxides on the surface of MCS.

2 Materials and Methods

2.1 Arsenic Solution

Arsenic was studied under the trivalent As(III) oxidation state as the more toxic form of As. As(III) stock solution (1 g/L) was prepared using sodium arsenite ($NaAsO_2$) that was purchased from Fisher Scientific, USA. All solutions were prepared by using ultra-pure water (18.2 MΩ cm, Direct-Q UV, Millipore, USA). The concentration of As(III) in the solution was determined using an atomic absorption spectrometer coupled with a continuous flow vapor generator (VGA-AAS; VP100, Thermo Scientific, USA).

2.2 Biosorbent Preparation

The CS was collected from a local agricultural field in Saskatchewan, washed with tap water, dried at 60 °C, before being ground, and sieved (400–840 μm). The MCS was prepared based on the optimized procedure reported by [27]. Briefly, 5 g CS was immersed in a 0.15 M $FeCl_3$ solution and sonicated for 30 min. Then the iron was precipitated by dropwise addition of 10 M NaOH solution and adjusting the final pH to 3 under magnetic stirring. The stirrer was switched off, and the suspension was allowed to age for a day. Afterward, the created Fe oxide-loaded particles were filtered, washed using deionized water, dried at 60 °C for 24 h, and used for As(III) sorption experiments.

2.3 Biosorbent Characterization

The morphology and structure of the CS and MCS were characterized by field emission scanning electron microscopy (FE-SEM; Hitachi SU8010, Japan). Fourier transform infrared spectroscopy (FTIR) was used to investigate the functional groups of CS and MCS (Smith's Detection IlluminatIR FTIR microscope, USA). The crystallinity of the biosorbent was determined by a Rigaku Ultima IV X-Ray Diffractometer (Rigaku Americas Corp., USA). Brunauer–Emmett–Teller (BET) surface area of the biosorbent was determined by N_2 adsorption using an ASAP 2020 (Micromeritics, USA). The point of zero charge (pH_{PZC}) was determined using the pH drift method [28]. The Fe content of the MCS was determined using acid digestion followed by atomic absorption spectrometry (AAS, Thermo Scientific iCE 3000 series, USA) to verify the deposition of Fe oxide on the surface of MCS.

2.4 As(III) Sorption Experiments

2.4.1 Sorption Isotherms and Kinetics

Adsorption isotherms were determined in order to study the relation between the amount of As(III) in solution and the sorbed amount on the MCS. MCS (dosage of 1 g/L) was placed in contact with As(III) solutions with different initial concentrations ranging from 500 to 40,000 μg/L at 25 °C and stirred for 72 h at 200 RPM. Initial experiments indicated that the 72 h duration was adequate to achieve equilibrium. Four sorption isotherm models were used to fit the experimental equilibrium data of As(III) sorption to MCS, namely the Langmuir, Freundlich, Temkin, and Redlich–Peterson models. For the sorption kinetics experiments, As(III) sorption was evaluated as a function of time to determine the influence of contact time on sorption capacity at an initial As(III) concentration of 2500 μg/L. Four kinetics models (pseudo-first-order, pseudo-second-order, intra-particle diffusion, Elovich) were used to investigate the sorption mechanism, characteristic constants, and solid-phase sorption. The amount of As(III) sorbed per unit mass (q_t, mg/g) at any time t was calculated as (Eq. 1):

$$q_t = \frac{C_0 - C_t}{m} V \tag{1}$$

where C_0 is the initial concentration of As(III) in the solution (μg/L), C_t is the As(III) concentration in solution at any time (t) (μg/L), V is the volume of the solution (L), and m is the mass of the biosorbent (g).

2.4.2 Effect of pH and Co-existing Ions

In order to study the effect of the initial pH of the solution, the sorption experiments were conducted at a pH range of 3–10 at an initial As(III) concentration of 2500 μg/L, constant MCS suspension density of 1 g/L, and a temperature of 25 °C. Initial solution pH was adjusted by dropwise addition of 0.1 M HCl or NaOH solutions. The effect of different co-existing ions in water including selenite (SeO_3^{2-}), selenate (SeO_4^{2-}), phosphate (PO_4^{3-}), nitrate (NO_3^-), and chloride (Cl^-) on the removal of As(III) was investigated by increasing the concentration of co-existing ions from 0 to 10 mg/L at a fixed As(III) concentration of 2500 μg/L.

3 Results and Discussion

3.1 Biosorbent Characterization

The surface morphological characteristics of the CS and MCS are presented in the SEM images (Fig. 1). These images indicate the relatively rougher structure of MCS (Fig. 1b) as compared to CS (Fig. 1a). While the surface of CS is smooth, the surface of the MCS is rough, indicating deposition of a Fe oxide layer on the biomass surface. The Fe oxide deposition was confirmed by measuring the Fe content of the MCS, which indicated the deposition of 74.8 mg Fe per gram of MCS. In addition, the BET surface area of the CS increased from 2.0 to 3.0 m^2/g after modification, which can increase the adsorptive surface area and subsequently provide more active As(III) sorption sites [29].

FTIR spectroscopy (wavenumber range of 4000–650 cm^{-1}) revealed no significant change in the functional groups upon modification of CS (Fig. 2a). However, both spectra showed the presence of cellulose, hemicellulose, and lignin in the materials [30]. The bands at ~ 834 and ~ 895 cm^{-1} can be associated with aromatic C–H

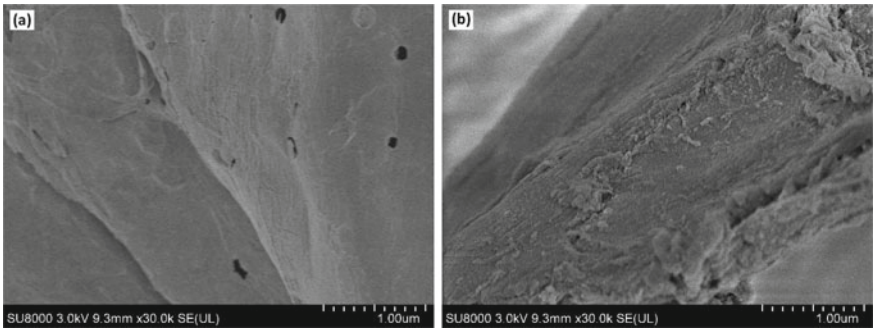

Fig. 1 SEM images of, **a** canola straw (CS), **b** modified canola straw (MCS)

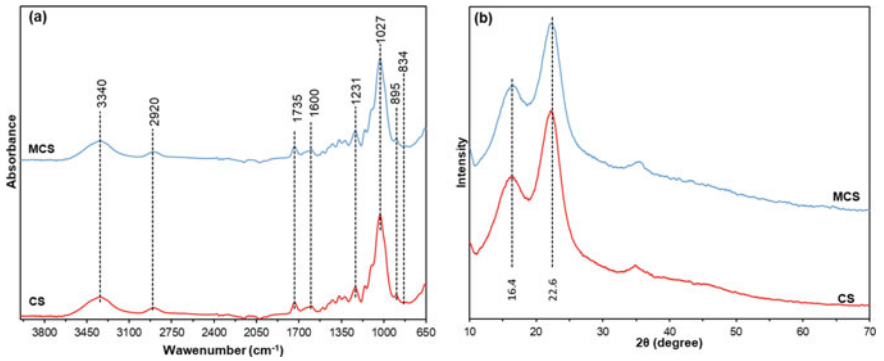

Fig. 2 **a** FTIR spectra and **b** XRD pattern of canola straw (CS) and modified canola straw (MCS)

present in lignin [31], and C–O–C rings in cellulose [32], respectively. The band at ~ 1027 cm^{-1} can be attributed to the C–O in cellulose, and the band at ~ 1231 cm^{-1} can be assigned to the C–OH of the phenolic groups [33]. The spectral peak at ~ 1600 cm^{-1} can be related to aromatic skeletal vibrations and C = O stretches present in the aromatic structure of the lignin. The band at ~ 1735 cm^{-1} can be assigned to the acetyl groups in hemicellulose [34]. The band at ~ 2920 cm^{-1} can be attributed to CH_2 and CH_3 groups in cellulose, hemicellulose, and lignin [30], and the broad peak at ~ 3340 can be due to –OH surface functional groups [35].

The XRD patterns were in good agreement with the FTIR spectra (Fig. 2b). The CS and MCS showed similar broad peaks at 2θ values of 16.4 and 22.6°, which can be attributed to cellulose [36]. However, the XRD pattern of the MCS lacks any diffraction peak indicating the amorphous nature of the deposited Fe oxides. These results are in agreement with the previous results indicating the formation of amorphous Fe oxide under low pH and drying conditions [37, 38]. FeOOH will be the dominant Fe oxide phase in the modification condition that can be deposited on the surface of CS (Eq. 2) [39]:

$$Fe^{3+} + 3OH^{-} \leftrightarrow FeOOH \downarrow + H_2O. \quad (2)$$

3.2 Sorption Isotherms and Kinetics

Sorption isotherms can be used to describe the interaction between the sorbate and the sorbent. Equilibrium sorption results indicated that the amount of sorbed As(III) increased from 407 to 6407 μg/g by increasing the initial As(III) concentration from 500 to 20,000 μg/L. The maximum As(III) sorption capacity of 6407 μg/g is comparable with the reported values for other Fe treated biomasses such as 1400 μg/g for *Melia azedarach* sawdust [40], 4370 μg/g for hazelnut shells [41], 9740 μg/g

for pinecone [42], and 12,600 for jute fibers [21]. Overall, it is clear that the MCS developed in the current study performed well overall.

Four isotherm models were used to describe the sorption behavior of As(III) on MCS. The linearized isotherm models were fitted with the experimental data (Fig. 3a), and the estimated isotherm coefficients are shown in Table 1. It is observed from Fig. 3a and the R^2 values that the data fitted better to the Freundlich (0.99) and Redlich–Peterson (0.99) isotherm models than the Langmuir (0.97) and Temkin (0.89) models. The Langmuir model assumes that sorption is monolayer and surface-active sites have uniform energy. In contrast to Langmuir, the Freundlich model assumes that the sorbent surface energy is heterogeneous and the sorption process is multilayer [43]. The Temkin model assumes sorption energy decreases linearly with increasing sorption quantity [44]. Lastly, the Redlich–Peterson model is a three-parameter model that incorporates features of both the Langmuir and Freundlich models. This model assumes a hybrid sorption mechanism and approaches the ideal Langmuir condition when the exponent β is close to 1 and resembles the Freundlich model if values of β are close to zero [45]. Therefore, considering the R^2 values and the value of $0 < \beta(0.56) < 1$ (Table 1), a hybrid sorption mechanism took place in biosorption of As(III) using MCS. In addition, the value of n in the Freundlich model ($n_{fr} = 2.05$) indicated that the sorption process was favorable. Generally, when $0 < 1/n < 1$, the sorption is considered to be favorable, and when $1/n > 1$, the sorption is considered to be unfavorable [46].

The kinetic experiments of As(III) removal were carried out to understand the sorption behavior of MCS. The contact time was varied between 0 and 4320 min (72 h) to establish equilibrium. The As(III) sorption rate was fast, with 66% of the ultimate sorption occurring in the first 4 h, and the sorption capacity continued to increase for the next 72 h with a lower sorption rate to approach equilibrium (Fig. 3b). The sorption kinetics were best modeled by pseudo-second-order ($R^2 = 0.99$) and Elovich ($R^2 = 0.98$) models than the pseudo-first-order ($R^2 = 0.95$) and intra-particle diffusion models ($R^2 = 0.82$) (Table 1). The high correlation coefficient of the pseudo-second-order model suggested that the overall mechanism of sorption

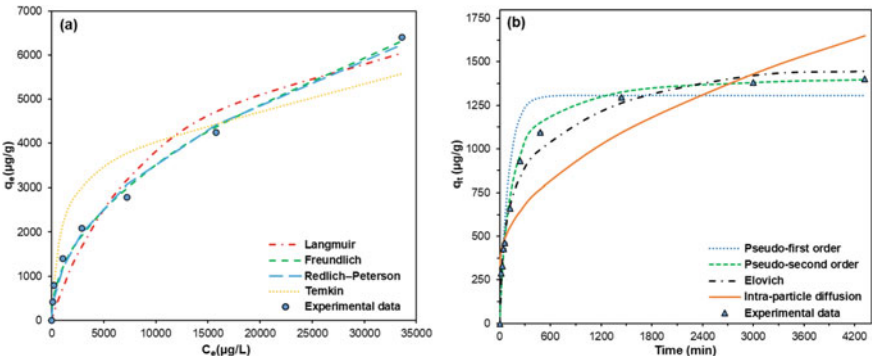

Fig. 3 **a** Biosorption isotherm, **b** biosorption kinetics for As(III) using MCS

Table 1 Results of the isotherm and kinetic models, equations, and estimated parameters for biosorption of As(III) by MCS

Model	Equation	Parameter	Value
Isotherm			
Langmuir	$q_e = \frac{K_L q_{\max} C_e}{1+K_L C_e}$	$q_{\max}$ (μg/g) K_L (L/mg) R^2	8077 0.089 0.97
Freundlich	$q_e = K_F C_e^{\frac{1}{n}}$	K_{Fr} (μg/g)(L/μg)$^{1/\mathrm{nFr}}$ n_{Fr} R^2	39.0 2.05 0.99
Temkin	$q_e = \frac{\mathrm{RT}}{b_T}\ln(K_T C_e)$	K_T (L/mg) b_T R^2	12.1 845 0.89
Redlich–Peterson	$q_e = \frac{K_{\mathrm{RP}} C_e}{1+a_{\mathrm{RP}} C_e^{\beta}}$	K_{RP} (L/g) a_{RP} (L/μg)$^{\beta}$ β R^2	6.3 0.091 0.56 0.99
Kinetics			
Pseudo-first-order	$q_t = q_e\left(1 - e^{-k_1 t}\right)$	k_1 (1/min) q_e exp. (μg/g) q_e cal. (μg/g) R^2	0.01 1404 1307 0.95
Pseudo-second-order	$\frac{t}{q_t} = \frac{1}{k_2 q_e^2} + \left(\frac{1}{q_e}\right)t$	k_2 (g/μg.min) q_e cal. (μg/g) R^2	5.8e-6 1436.7 0.99
Intra-particle diffusion	$q_t = k_p t^{1/2} + C$	k_p (μg/g.min$^{0.5}$) C (μg/g) R^2	56.3 905.3 0.82
Elovich	$q_t = \frac{1}{b}\ln(1 + abt)$	a (μg/g.min) b (kg/m) R^2	35.2 4.3 0.98

of As(III) onto MCS was controlled by a chemisorption process [47]. The intra-particle diffusion model failed to describe the experimental kinetic data indicating that the intra-particle-diffusion was not the only rate-limiting step. The validity of the Elovich model suggested that the chemisorption mechanism (e.g., surface complexation) is likely the main rate-determining step for the sorption which is in agreement with the pseudo-second-order model.

3.3 Effect of pH

The pH of solution is an important factor in the As(III) sorption process because both the speciation of As ions in an aqueous solution and the surface charge of the

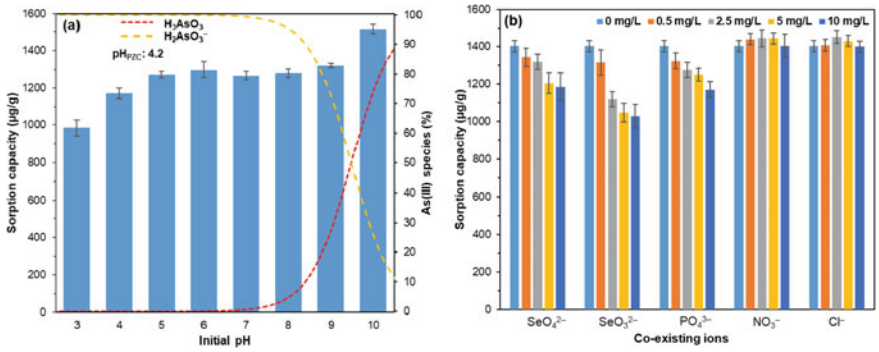

Fig. 4 Impacts to As(III) sorption capacity of MCS: **a** initial pH; **b** co-existing ions

biosorbent are pH dependent [16]. The speciation of As(III) species and equilibrium constants are shown below (Eq. 3) [48]:

$$\begin{aligned} H_3AsO_3 &\leftrightarrow H_2AsO_3^- + H^+ \quad pK_{a1} = 9.3 \\ H_2AsO_3^- &\leftrightarrow HAsO_3^{2-} + H^+ \quad pK_{a2} = 12.1 \\ HAsO_3^{2-} &\leftrightarrow AsO_3^{3-} + H^+ \quad pK_{a2} = 12.7 \end{aligned} \tag{3}$$

Based on the pK_a values in Eq. 3, As(III) exists mainly as neutral H_3AsO_3 at pH values lower than 9.2, and $H_2AsO_3^-$ becomes dominant at pH values above 9.2 (Fig. 4a).

The effect of the initial pH of solution on the removal As(III) by MCS was investigated (Fig. 4a). The interaction between As(III) species and the surface of the MCS was influenced by solution pH, and the solution pH had a significant effect on As(III) sorption capacity of MCS ($p < 0.01$). As the pH increased from 3 to 6, the As(III) sorption capacity increased from 984 to 1298 μg/g and remained relatively constant between pH 6 and 9 (ranged between 1266 and 1320 μg/g) before reaching a maximum value of 1515 μg/g at pH 10. Previously, similar sorption behaviors have been reported for As(III) on Fe oxides surfaces [49, 50]. The determined pH_{pzc} of the MCS was 4.2. Considering that at the pH values lower than 4.2 As(III) exists as neutral species (H_3AsO_3, and the sorption capacity of MCS was the lowest at low pH values; thus, the electrostatic attraction was not responsible for As(III uptake. The enhanced sorption capacity at $5 < pH < 9$ can be attributed to outer-sphere complexation or inner-sphere complexation of As(III with Fe oxides on the biosorbent surface [51]. The higher As(III) sorption capacity at pH 10 can be attributed to the stronger interaction between the deposited Fe oxides on the surface of MCS and As(III) ions. It has been reported that As(III) is sorbed more strongly at alkaline conditions, and in general, the maximum anion sorption occurs at pH values in the pK_a range of the conjugate acid (currently the $pK_{a1} = 9.3$ for arsenious acid) (Eq. 3) [52, 53].

3.4 Effect of Co-existing Anions

Given that some anions in natural waters and anthropogenic wastewaters may compete with As(III) for the sorption sites on the MCS surface, investigating the possible competition between As(III) and examples of these anions is necessary. Therefore, the effect of different anions (Cl^-, NO_3^-, PO_4^{3-}, SeO_3^{2-}, SeO_4^{2-}) on the biosorption of As(III) on MCS was investigated (Fig. 4b). The presence of Cl^- and NO_3^- did not have a significant effect ($p > 0.05$) on the adsorption of As(III) when the concentration of the co-existing ions varied from 0 to 10 mg/L. However, the removal of As(III) was affected significantly ($p < 0.01$) in the presence of PO_4^{3-}, SeO_3^{2-}, SeO_4^{2-}. With an increase in the concentration of ions from 0 to 10 mg/L, the As(III) sorption capacity decreased from 1404 to 1171, 1028, and 1186 μg/g in the presence of PO_4^{3-}, SeO_3^{2-}, and SeO_4^{2-}, respectively.

It has been reported that Cl^- and NO_3^- could only bind weakly to the surface of metal oxides by forming an outer-sphere complex [54, 55]. Generally, outer-sphere complexation is significantly affected by ionic strength and decreases with increasing ionic strength. Conversely, in the case of inner-sphere surface complexation, sorption capacity increases (or stays constant) with increasing ionic strength [56]. Considering that increase of Cl^- and NO_3^- concentrations did not influence the As(III) sorption capacity, the dominant mechanism of As(III) sorption onto the MCS can be attributed to inner-sphere surface complexation. On the other hand, PO_4^{3-} and SeO_3^{2-} bind strongly to metal oxides by forming inner-sphere complexes, and SeO_4^{2-} forms both relatively weaker inner- and outer-sphere complexes [55, 57]. Therefore, the impact of PO_4^{3-} and SeO_3^{2-} on As(III) sorption will be stronger than SeO_4^{2-}, which is in line with the amount of reduction in As(III) sorption capacity in the presence of PO_4^{3-} (233 μg/g) and SeO_3^{2-} (376 μg/g), and SeO_4^{2-} (218 μg/g).

Therefore, based on the results of sorption experiments and the effect of co-existing ions on the As(III) scorpion capacity of MCS, it can be deduced that inner-sphere complexation is the main As(III) sorption mechanism. The inner-sphere complexation of As(III) with Fe oxides on the surface of MCS may take place by three complexation types, including mononuclear-monodentate, binuclear-bidentate, and mononuclear-bidentate complexes (Fig. 5).

3.5 Conclusion

The current study showed the viability of using Fe-modified canola straw (MCS) for the removal of As(III) from water. According to the results, the maximum As(III) sorption capacity of the MCS compares favorably to other similar sorbents in the literature. The Freundlich and Redlich–Peterson isotherm models were best-fitted to equilibrium data suggesting that a hybrid sorption mechanism took place in the removal of As(III) using MCS. Adsorption kinetics were well described by pseudo-second-order and Elovich models indicating the chemisorption nature of the process.

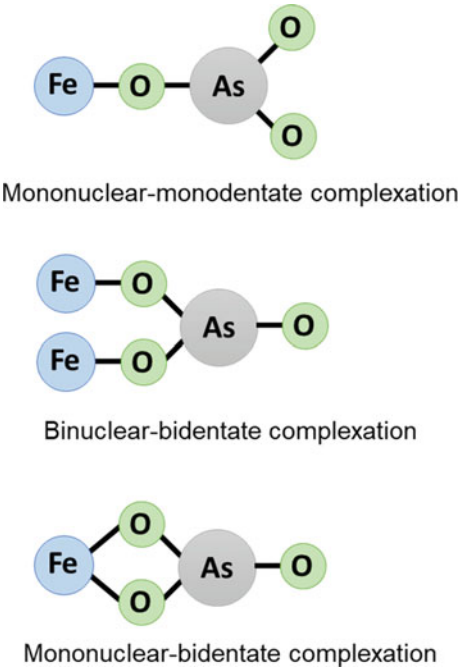

Fig. 5 Possible inner-sphere surface complexes of As(III) formed on the surface of MCS

As(III) uptake by MCS increased with increasing pH from 3 to 5, remained constant in the pH range of 5–9, and reached a maximum of 1515 μg/g at pH 10. Studying the inhibition effects of co-existing ions on As(III) sorption showed an insignificant effect of Cl^- and NO_3^-, while the effects of other ions were in the following order: $SeO_3^{2-} > PO_4^{3-} > SeO_4^{2-}$. Based on the sorption experiment results, inner-sphere complexation can be the main mechanism of As(III) sorption on MCS. While the batch adsorption experiments showed the promising potential of the MCS for As(III) sorption, further experiments are required to study the stability of the sorbent in the long-term adsorption process, identify a proper desorption agent, and investigate the regeneration-reuse capability of the adsorbent.

Funding The research was financially supported by the Saskatchewan Agriculture Development Fund and two NSERC Discovery Grants (K. McPhedran and J. Soltan). Kh. Zoroufchi Benis is supported by the Vanier Canada Graduate Scholarship and Saskatchewan Opportunity Scholarship.

References

1. Chappells H, Parker L, Fernandez CV, Conrad C, Drage J, O'Toole G, Campbell N, Dummer TJB (2014) Arsenic in private drinking water wells: an assessment of jurisdictional regulations and guidelines for risk remediation in North America. J Water Health 12:372–392. https://doi.org/10.2166/wh.2014.054
2. Shakoor MB, Niazi NK, Bibi I, Shahid M, Sharif F, Bashir S, Shaheen SM, Wang H, Tsang DCW, Ok YS, Rinklebe J (2018) Arsenic removal by natural and chemically modified water melon rind in aqueous solutions and groundwater. Sci Total Environ 645:1444–1455. https://doi.org/10.1016/J.SCITOTENV.2018.07.218
3. Sadeghi F, Nasseri S, Yunesian M, Nabizadeh R, Mosaferi M, Mesdaghinia A (2018) Carcinogenic and non-carcinogenic risk assessments of arsenic contamination in drinking water of Ardabil city in the Northwest of Iran. J Environ Sci Heal Part A 53:421–429. https://doi.org/10.1080/10934529.2017.1410421
4. Zhou Z, Liu Y, Liu S, Liu H, Zeng G, Tan X, Yang C, Ding Y, Yan Z, Cai X (2017) Sorption performance and mechanisms of arsenic(V) removal by magnetic gelatin-modified biochar. Chem Eng J 314:223–231. https://doi.org/10.1016/J.CEJ.2016.12.113
5. WHO (2011) Guidelines for drinking-water quality, 4th edn. World-Health-Organization, pp 315–318
6. Huq ME, Fahad S, Shao Z, Sarven MS, Al-Huqail AA, Siddiqui MH, Habib ur Rahman M, Khan IA, Alam M, Saeed M, Rauf A, Basir A, Jamal Y, Khan SU (2019) High arsenic contamination and presence of other trace metals in drinking water of Kushtia district, Bangladesh. J Environ Manag 242:199–209. https://doi.org/10.1016/J.JENVMAN.2019.04.086
7. Zoroufchi Benis K, Soltan J, McPhedran KN (2022) A novel method for fabrication of a binary oxide biochar composite for oxidative adsorption of arsenite: characterization, adsorption mechanism and mass transfer modeling. J Clean Prod 131832. https://doi.org/10.1016/J.JCLEPRO.2022.131832
8. Kumar ASK, Jiang S-J (2016) Chitosan-functionalized graphene oxide: a novel adsorbent an efficient adsorption of arsenic from aqueous solution. J Environ Chem Eng 4:1698–1713. https://doi.org/10.1016/j.jece.2016.02.035
9. Sogaard E (2014) Chemistry of advanced environmental purification processes of water: fundamentals and applications. Newnes
10. Zoroufchi Benis K, Motalebi Damuchali A, McPhedran KN, Soltan J (2020) Treatment of aqueous arsenic—a review of biosorbent preparation methods. J Environ Manage 273:111126. https://doi.org/10.1016/j.jenvman.2020.111126
11. Zoroufchi Benis K, Damuchali AM, Soltan J, McPhedran KN (2020) Treatment of aqueous arsenic—a review of biochar modification methods. Sci Total Environ. https://doi.org/10.1016/j.scitotenv.2020.139750
12. Roy P, Dey U, Chattoraj S, Mukhopadhyay D, Mondal NK (2017) Modeling of the adsorptive removal of arsenic(III) using plant biomass: a bioremedial approach. Appl Water Sci 7:1307–1321. https://doi.org/10.1007/s13201-015-0339-2
13. Siddiqui SI, Chaudhry SA (2017) Iron oxide and its modified forms as an adsorbent for arsenic removal: a comprehensive recent advancement. Process Saf Environ Prot. https://doi.org/10.1016/j.psep.2017.08.009
14. De D, Aniya V, Satyavathi B (2019) Application of an agro-industrial waste for the removal of As(III) in a counter-current multiphase fluidized bed. Int J Environ Sci Technol 16:279–294. https://doi.org/10.1007/s13762-018-1651-9
15. Vieira BRC, Pintor AMA, Boaventura RAR, Botelho CMS, Santos SCR (2017) Arsenic removal from water using iron-coated seaweeds. J Environ Manag 192:224–233. https://doi.org/10.1016/J.JENVMAN.2017.01.054
16. Zoroufchi Benis K, Soltan J, McPhedran KN (2021) Electrochemically modified adsorbents for treatment of aqueous arsenic: pore diffusion in modified biomass vs. biochar. Chem Eng J 423:130061. https://doi.org/10.1016/j.cej.2021.130061

17. Abid M, Niazi NK, Bibi I, Farooqi A, Ok YS, Kunhikrishnan A, Ali F, Ali S, Igalavithana AD, Arshad M (2016) Arsenic(V) biosorption by charred orange peel in aqueous environments. Int J Phytorem 18:442–449. https://doi.org/10.1080/15226514.2015.1109604
18. Ebrahimi R, Maleki A, Shahmoradi B, Daraei H, Mahvi AH, Barati AH, Eslami A (2013) Elimination of arsenic contamination from water using chemically modified wheat straw. Desalin Water Treat 51:2306–2316. https://doi.org/10.1080/19443994.2012.734675
19. Bowell RJ, Alpers CN, Jamieson HE, Nordstrom DK, Majzlan J (2014) The environmental geochemistry of arsenic—an overview. Rev Mineral Geochem 79:1–16. https://doi.org/10.2138/rmg.2014.79.1
20. Tian Y, Wu M, Lin X, Huang P, Huang Y (2011) Synthesis of magnetic wheat straw for arsenic adsorption. J Hazard Mater 193:10–16. https://doi.org/10.1016/J.JHAZMAT.2011.04.093
21. Hao L, Zheng T, Jiang J, Hu Q, Li X, Wang P (2015) Removal of As(III) from water using modified jute fibres as a hybrid adsorbent. RSC Adv 5:10723–10732. https://doi.org/10.1039/c4ra11901k
22. Meng F, Yang B, Wang B, Duan S, Chen Z, Ma W (2017) Novel dendrimerlike magnetic biosorbent based on modified orange peel waste: adsorption-reduction behavior of arsenic. ACS Sustain Chem Eng 5:9692–9700. https://doi.org/10.1021/acssuschemeng.7b01273
23. Canola Council (2022) Grown on Canadian farms, consumed around the world [WWW Document]. https://www.canolacouncil.org/about-canola/industry/
24. Saskcanola (2022) The Canola Story [WWW Document]. https://www.saskcanola.com/about/story.php
25. Yousefi H (2009) Canola straw as a bio-waste resource for medium density fiberboard (MDF) manufacture. Waste Manag 29:2644–2648. https://doi.org/10.1016/J.WASMAN.2009.06.018
26. Pronyk C, Mazza G (2012) Fractionation of triticale, wheat, barley, oats, canola, and mustard straws for the production of carbohydrates and lignins. Bioresour Technol 106:117–124. https://doi.org/10.1016/j.biortech.2011.11.071
27. Zoroufchi Benis K, Shakouri M, McPhedran K, Soltan J (2020) Enhanced arsenate removal by Fe-impregnated canola straw: assessment of XANES solid-phase speciation, impacts of solution properties, sorption mechanisms, and evolutionary polynomial regression (EPR) models. Environ Sci Pollut Res. https://doi.org/10.1007/s11356-020-11140-0
28. Alchouron J, Navarathna C, Chludil HD, Dewage NB, Perez F, Hassan EB, Pittman CU Jr, Vega AS, Mlsna TE (2020) Assessing South American *Guadua chacoensis* bamboo biochar and Fe3O4 nanoparticle dispersed analogues for aqueous arsenic(V) remediation. Sci Total Environ 706:135943. https://doi.org/10.1016/j.scitotenv.2019.135943
29. Jung K-W, Jeong T-U, Kang H-J, Chang J-S, Ahn K-H (2016) Preparation of modified-biochar from Laminaria japonica: Simultaneous optimization of aluminum electrode-based electro-modification and pyrolysis processes and its application for phosphate removal. Bioresour Technol 214:548–557. https://doi.org/10.1016/j.biortech.2016.05.005
30. Gautam SB, Alam MS, Kamsonlian S (2017) Adsorptive removal of As(III) from aqueous solution by raw coconut husk and iron impregnated coconut husk: kinetics and equilibrium analyses. Int J Chem React Eng 15. https://doi.org/10.1515/ijcre-2016-0097
31. Huang Z, Liang X, Hu H, Gao L, Chen Y, Tong Z (2009) Influence of mechanical activation on the graft copolymerization of sugarcane bagasse and acrylic acid. Polym Degrad Stab 94:1737–1745. https://doi.org/10.1016/j.polymdegradstab.2009.06.023
32. Qu G, Huang X, Yin Q, Ning P (2014) Dissolution of garlic stem in the 1-butylrpridinium bromide ionic liquid. J Chem Eng Jpn 47:435–441. https://doi.org/10.1252/jcej.13we163
33. Nadeem R, Manzoor Q, Iqbal M, Nisar J (2016) Biosorption of Pb(II) onto immobilized and native *Mangifera indica* waste biomass. J Ind Eng Chem 35:185–194. https://doi.org/10.1016/j.jiec.2015.12.030
34. Baker MJ, Trevisan J, Bassan P, Bhargava R, Butler HJ, Dorling KM, Fielden PR, Fogarty SW, Fullwood NJ, Heys KA, Hughes C, Lasch P, Martin-Hirsch PL, Obinaju B, Sockalingum GD, Sulé-Suso J, Strong RJ, Walsh MJ, Wood BR, Gardner P, Martin FL (2014) Using Fourier transform IR spectroscopy to analyze biological materials. Nat Protoc 9:1771–1791. https://doi.org/10.1038/nprot.2014.110

35. Niazi NK, Bibi I, Shahid M, Ok YS, Shaheen SM, Rinklebe J, Wang H, Murtaza B, Islam E, Farrakh Nawaz M, Lüttge A (2018) Arsenic removal by Japanese oak wood biochar in aqueous solutions and well water: Investigating arsenic fate using integrated spectroscopic and microscopic techniques. Sci Total Environ 621:1642–1651. https://doi.org/10.1016/J.SCITOTENV.2017.10.063
36. Dymińska L, Gągor A, Hanuza J, Kulma A, Preisner M, Zuk M, Szatkowski M, Szopa J (2014) Spectroscopic characterization of genetically modified flax fibers. J Mol Struct 1074:321–329. https://doi.org/10.1016/j.molstruc.2014.06.013
37. El-Moselhy MM, Ates A, Çelebi A (2017) Synthesis and characterization of hybrid iron oxide silicates for selective removal of arsenic oxyanions from contaminated water. J Colloid Interface Sci 488:335–347. https://doi.org/10.1016/J.JCIS.2016.11.003
38. Zeng L (2004) Arsenic adsorption from aqueous solutions on an Fe(III)-Si binary oxide adsorbent. Water Qual Res J Can 39:267–275. https://doi.org/10.2166/wqrj.2004.037
39. Zeng L (2003) A method for preparing silica-containing iron(III) oxide adsorbents for arsenic removal. Water Res 37:4351–4358. https://doi.org/10.1016/S0043-1354(03)00402-0
40. Davodia M, Alidadib H, Ramezanib A, Jamali-Behnamc F, Bonyadib Z (2019) Study of the removal efficiency of arsenic from aqueous solutions using Melia azedarach sawdust modified with FeO: isotherm and kinetic studies. Desalin Water Treat 137:292–299
41. Sert S, Celik A, Tirtom VN (2017) Removal of arsenic (III) ions from aqueous solutions by modified hazelnut shell. Desalin Water Treat 75:115–123
42. Pholosi A, Naidoo BE, Ofomaja AE (2018) Clean application of magnetic biomaterial for the removal of As(III) from water. Environ Sci Pollut Res 25:30348–30365. https://doi.org/10.1007/s11356-018-2990-2
43. Singh P, Pal P, Mondal P, Saravanan G, Nagababu P, Majumdar S, Labhsetwar N, Bhowmick S (2021) Kinetics and mechanism of arsenic removal using sulfide-modified nanoscale zerovalent iron. Chem Eng J 128667. https://doi.org/10.1016/j.cej.2021.128667
44. Zhuang H, Zhong Y, Yang L (2020) Adsorption equilibrium and kinetics studies of divalent manganese from phosphoric acid solution by using cationic exchange resin. Chin J Chem Eng 28:2758–2770. https://doi.org/10.1016/j.cjche.2020.07.029
45. Kim S, Gholamirad F, Yu M, Park CM, Jang A, Jang M, Taheri-Qazvini N, Yoon Y (2021) Enhanced adsorption performance for selected pharmaceutical compounds by sonicated Ti3C2TX MXene. Chem Eng J 406:126789. https://doi.org/10.1016/j.cej.2020.126789
46. Al-Ghouti MA, Da'ana DA (2020) Guidelines for the use and interpretation of adsorption isotherm models: a review. J Hazard Mater. https://doi.org/10.1016/j.jhazmat.2020.122383
47. Xiang L, Niu CG, Tang N, Lv XX, Guo H, Li ZW, Liu HY, Lin LS, Yang YY, Liang C (2020) Polypyrrole coated molybdenum disulfide composites as adsorbent for enhanced removal of Cr(VI) in aqueous solutions by adsorption combined with reduction. Chem Eng J 408:127281. https://doi.org/10.1016/j.cej.2020.127281
48. Yu X, Tong S, Ge M, Zuo J, Cao C, Song W (2012) One-step synthesis of magnetic composites of cellulose@iron oxide nanoparticles for arsenic removal. J Mater Chem A 1:959–965. https://doi.org/10.1039/C2TA00315E
49. Pervez MN, Fu D, Wang X, Bao Q, Yu T, Naddeo V, Tian H, Cao C, Zhao Y (2021) A bifunctional α-FeOOH@GCA nanocomposite for enhanced adsorption of arsenic and photo Fenton-like catalytic conversion of As(III). Environ Technol Innov 22:101437. https://doi.org/10.1016/J.ETI.2021.101437
50. Yu F, Sun S, Ma J, Han S (2015) Enhanced removal performance of arsenate and arsenite by magnetic graphene oxide with high iron oxide loading. Phys Chem Chem Phys 17:4388–4397. https://doi.org/10.1039/C4CP04835K
51. Zubair YO, Fuchida S, Tokoro C (2020) Insight into the mechanism of arsenic(III/V) uptake on mesoporous zerovalent iron-magnetite nanocomposites: adsorption and microscopic studies. ACS Appl Mater Interfaces 12:49755–49767. https://doi.org/10.1021/ACSAMI.0C14088/SUPPL_FILE/AM0C14088_SI_001.PDF
52. Brechbühl Y, Christl I, Elzinga EJ, Kretzschmar R (2012) Competitive sorption of carbonate and arsenic to hematite: combined ATR-FTIR and batch experiments. J Colloid Interface Sci 377:313–321. https://doi.org/10.1016/J.JCIS.2012.03.025

53. Manning BA, Fendorf SE, Goldberg S (1998) Surface structures and stability of arsenic(III) on goethite: spectroscopic evidence for inner-sphere complexes. Environ Sci Technol 32:2383–2388. https://doi.org/10.1021/ES9802201
54. Ma Z, Shan C, Liang J, Tong M (2018) Efficient adsorption of Selenium(IV) from water by hematite modified magnetic nanoparticles. Chemosphere 193:134–141. https://doi.org/10.1016/j.chemosphere.2017.11.005
55. Xin Y, Gu P, Long H, Meng M, Yaseen M, Su H (2021) Fabrication of ferrihydrite-loaded magnetic sugar cane bagasse charcoal adsorbent for the adsorptive removal of selenite from aqueous solution. Colloids Surf A: Physicochem Eng Aspects 614:126131. https://doi.org/10.1016/j.colsurfa.2020.126131
56. Zoroufchi Benis K, McPhedran KN, Soltan J (2022) Selenium removal from water using adsorbents: a critical review. J Hazard Mater 424:127603. https://doi.org/10.1016/J.JHAZMAT.2021.127603
57. Zhang N, Lin LS, Gang D (2008) Adsorptive selenite removal from water using iron-coated GAC adsorbents. Water Res 42:3809–3816. https://doi.org/10.1016/J.WATRES.2008.07.025